FINAL PUBLISHABLE REPORT

Grant Agreement number	17IND08
Project short name	AdvanCT
Project full title	Advanced Computed Tomography for dimensional and surface measurements in industry

Project start date and duration:	01 June 2018, 42 months	
Coordinator: Ulrich Neuschaefer-Rube, PTB Tel: +49 31 592 5311 E-mail: ulrich-neuschaefer-rube@ptb.de Project website address: www.ptb.de/empir2018/advanct		
Internal Funded Partners: 1 PTB, Germany 2 BAM, Germany 3 DTI, Denmark 4 FSB, Croatia 5 LNE, France 6 METAS, Switzerland 7 NPL, United Kingdom 8 VTT, Finland	External Funded Partners: 9 CEA, France 10 Empa, Switzerland 11 FAU, Germany 12 UBATH, United Kingdom 13 UNOTT, United Kingdom 14 UoS, United Kingdom	Unfunded Partners: 15 Bosch, Germany 16 LEGO, Denmark 17 NovoNordisk, Denmark 18 VG, Germany 19 Werth, Germany 20 Yxlon, Germany 21 Zeiss, Germany
RMG: -		

TABLE OF CONTENTS

1 Overview

Computed tomography (CT) is a contact-free measurement method which allows the complete geometry of objects to be determined. This includes the inner and outer geometry and the surface texture, all of which are typically not fully accessible by other measurement methods. There are a broad range of applications for CT, which include macro- and microfabrication, the automotive and telecom industries, and additive manufacturing.

In order to support future dimensional metrology in advanced manufacturing, this project developed traceable CT measurement techniques for dimensions and surface texture. In addition, current issues regarding traceability, measurement uncertainty, sufficient precision/accuracy, scanning time, multi-material, surface form and roughness, suitable reference standards, and simulation techniques were addressed by this project.

Within the framework of the project, significant progress was made in increasing the accuracy and traceability of CT measurements. New fields of application were opened up through the CT measurement of roughness and the reduction of scanning time.

2 Need

Over the past few years, CT has increasingly been used for dimensional measurements of both the inner and outer geometry of workpieces, such as cavities and parts in mounted assemblies. Such workpieces originate from macro- and microfabrication, the automotive and telecommunication industries, and additive manufacturing, thereby showing the potential broad use of CT.

Despite the rapidly increasing use of CT in industry, the measurement errors of most CT systems are too large and needed to be substantially reduced, i.e. by a factor of 2 – 8, to 10 µm even when measuring mid-size parts (approx. 1000 cm^3). However, the traceability of CT results needed to be established and methods to estimate the measurement uncertainty needed to be developed. Further to this, the time required to perform CT measurements and data evaluation needed to be reduced from hours to minutes if CT is to be more widely used in industry.

Guidelines and standards, such as standardised test procedures and specifications, are also needed to support a fair and competitive market and users of industrial CT. The German standardisation committee VDI/GMA 3.33 has developed some national guidelines (VDI/VDE 2630-series) for dimensional measurements using industrial CT. In addition, an international standard defining acceptance and reverification tests for CMS using the CT principle is currently under development by ISO TC213 Dimensional and geometrical product specifications and verification WG10 Coordinate measuring machines, which will become part of the ISO 10360-series. Therefore, this project supported these standardisation bodies by providing input to them on inline CT and multi-material measurements.

The above needs are underpinned by the EURAMET roadmap and Strategic Research Agenda and a report published by Frost and Sullivan in 2015 on “Strategic Analysis of Computed Tomography Technology in the Dimensional Metrology Market” In this report, the key areas identified for developing a broader use of industrial CT in industry are “Capabilities to improve measurement resolution”, “Support for multi-material complexity” and “Reduced measurement time (scanning and reconstruction)”.

3 Objectives

The overall goal of this project was to develop metrological capacity in Advanced Computed Tomography for dimensional and surface measurements in industry. The specific objectives of this project were:

1. To develop traceable and validated methods for absolute CT characterisation including the correction of geometry errors by 9 degrees of freedom (DoF). This included the development of reference standards, traceable calibration methods and thermal models for instrument geometry correction, as well as the correction of errors originating in the X-ray tube and the detector in order to improve CT accuracy.
2. To develop improved and traceable methods for dimensional CT measurements with a focus on measurements of sculptured / freeform surfaces, roughness, and multi-material effects including supplementary material characterisation.

3. To develop fast CT methods for inline applications based on improved evaluation of noisy, sparse, few, or limited angle X-ray projections, and reconstruction methods. This was undertaken using a reduced number of projections from well-known directions and include enhanced post-processing.
4. To develop traceable methods for uncertainty estimation using virtual CT models and Monte-Carlo simulations. Batch simulation and evaluation capacities was improved. The determination of accurate model parameters was necessary for a reliable uncertainty estimation and this was performed for different CTs and it was systematised. Corrections for several artefacts were developed. Uncertainty was estimated by Monte-Carlo based simulation and verified using the calibrated standards developed in WP1.
5. To facilitate the take up of the technology and measurement infrastructure developed in the project by the measurement supply chain (accredited laboratories, instrumentation manufacturers), standards developing organisations (e.g. ISO TC213 WG10, VDI-GMA 3.33 Technical Committee Computed Tomography in Dimensional Measurements) and end users (e.g. plastic manufacturers, automotive, telecommunication, medical and pharmaceutical industries and metrology service providers).

4 Results

Objective 1:

To develop traceable and validated methods for absolute CT characterisation including the correction of geometry errors by 9 degrees of freedom (DoF). This included the development of reference standards, traceable calibration methods and thermal models for instrument geometry correction, as well as the correction of errors originating in the X-ray tube and the detector in order to improve CT accuracy.

Reference standards

This project provides industry and the scientific community with methods to characterise CT geometry, either based on calibrated reference standards or traceable calibration measurements (e.g., interferometry). To this end, more than ten reference standards optimised for different tasks were developed, characterised, and provided to the consortium.

3D multi-sphere standards and 2D hole foils for CT geometry determination (Figure 1) were developed and calibrated by PTB, METAS, LNE, VTT, Werth with measurement uncertainties down to 100 nm. Using only two radiographs of a calibrated 2D hole foil is a fast and highly precise method of determining the geometrical scale factor of CT measurements. It has been validated successfully by BAM, METAS and PTB. The voxel sizes determined via this method were compared with voxel sizes determined from CT scans of calibrated objects. Relative errors between the voxel sizes in the range of 10^{-5} were achieved with minimal effort using cone-beam CT systems at moderate magnifications.

CT geometry determination using 3D multi-sphere standards was validated on an industrial CT system and compared to industrial state-of-the-art CT geometry calibration in collaboration between METAS and Yxlon. At the geometry calibration position, the multi-sphere standard was slightly more accurate ($< 10^{-5}$), however, when deviating from it the accuracy deteriorates rapidly. To overcome this limitation, a method employing a calibrated multi-sphere standard in combination with accurately measured shifts, realised using the CT system's linear axes, was developed and validated by METAS. This was especially important for dimensional measurements at high magnifications, where the geometry parameters have to be known to the micrometre level.

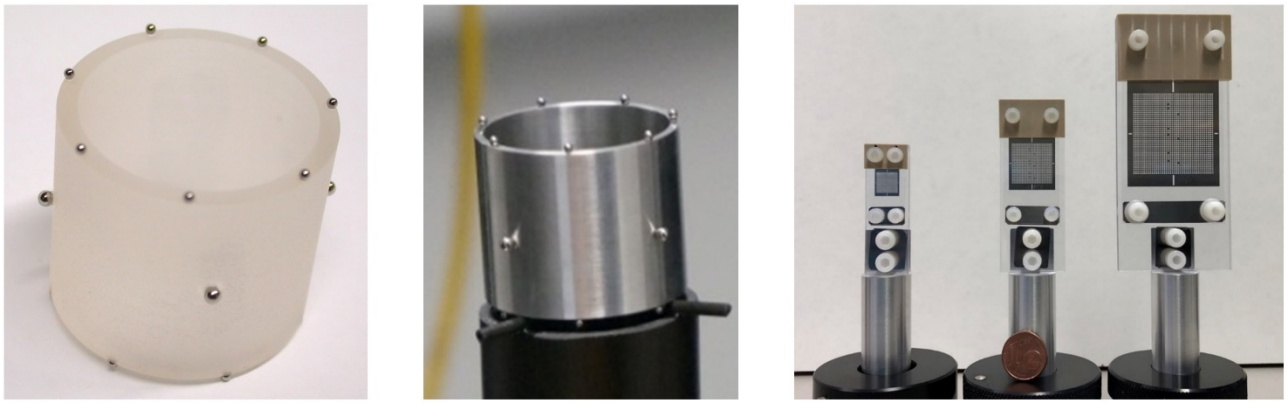

Figure 1: Selection of developed reference standards for CT geometry determination: Multi-sphere standards made from low-CTE ceramic and aluminium (left, METAS) and 2D hole foils made from Invar (right, PTB).

Reference standards with more complex geometries and consisting of multiple materials were developed, built and calibrated for CT performance evaluation by METAS, VTT, and LNE (Figure 2). They were used for measurement comparisons and to validate simulations.

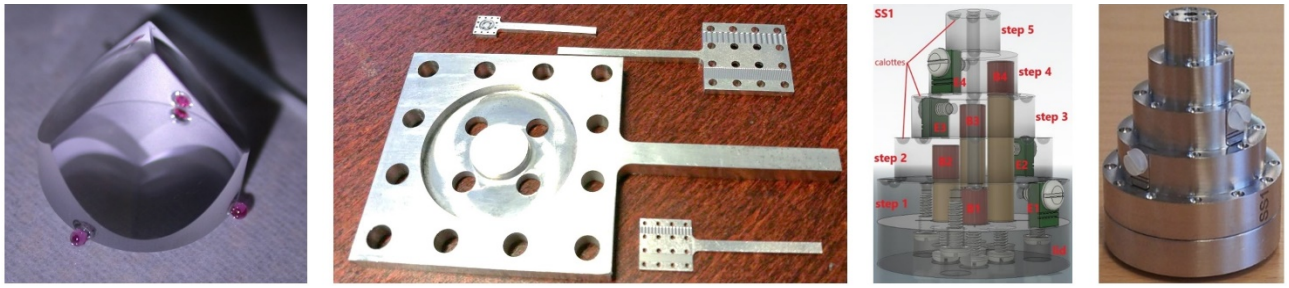

Figure 2: Selection of developed reference standards for CT performance evaluation.

Thermal characterisation and modelling

To study the influence of temperature variations on CT geometry, calibrated temperature measurement systems have been installed on two commercial and one research CT system at FAU, FSB, and METAS. Comprehensive characterisations (Figure 3) were used to develop effective mitigation strategies. These included recommendations for warm-up times for the CT system to reach thermal equilibrium and ameliorated water-cooling systems. Furthermore, the CT system at FSB was digitally twinned for numerical simulations. A full computational fluid dynamics model considered active water-cooling and ambient airflow. It enabled us to predict and account for drifts in CT geometry solely based on temperature measurements (Figure 4).

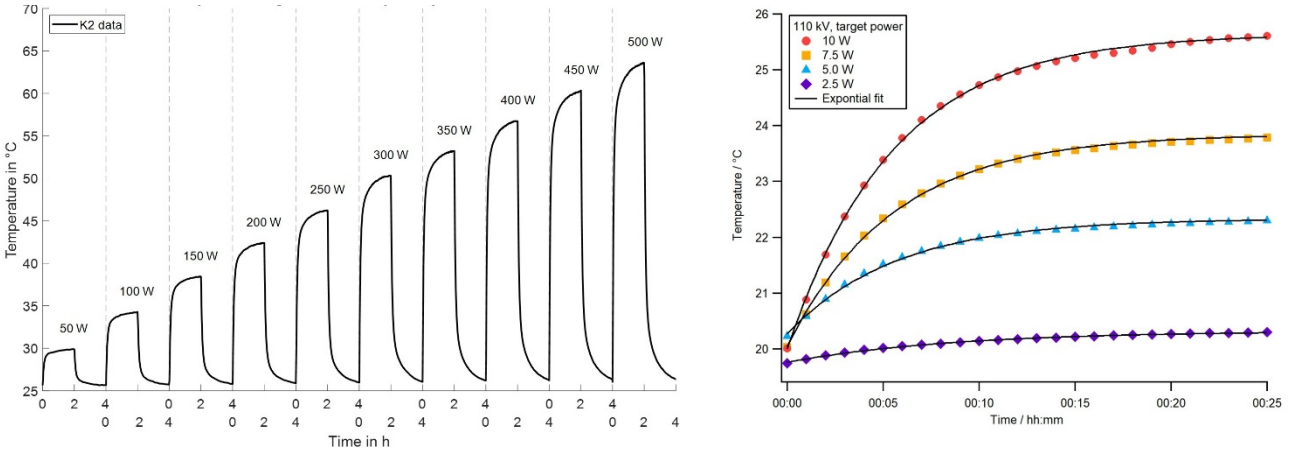

Figure 3: Temperature evolution of a reflection target X-ray tube with target power up to 500 W (left) and a transmission target X-ray tube up to 10 W (right) target power.

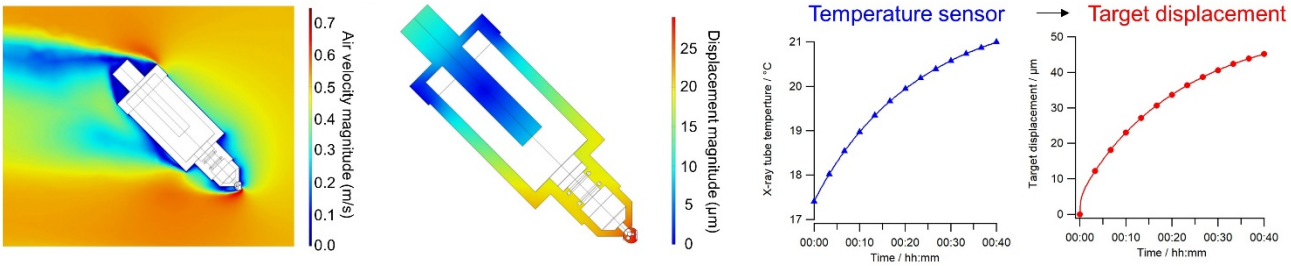

Figure 4: Numerical simulations of air-flow velocity around and temperature induced deformation of an X-ray tube. Thus, data from a temperature sensor enables the determination of geometrical displacements.

X-ray tube and detector specific effects

The influence of complex error sources, originating from the X-ray tube and the flat-panel detector were investigated and disseminated to relevant industries. The verification measurements at METAS and PTB were assisted by Zeiss and VG.

An optical X-ray tube measurement system was developed at METAS to account for the thermal expansion. Employing it, expansions of several micrometres were compensated to the sub-micrometre level. In addition, the complex thermal deformation of the transmission X-ray tube's target was numerically modelled and characterised by radiography and laser interferometry (Figure 5). The X-ray tube specific effects led to relative errors in the order of several 10^{-4} at high magnifications that could be reduced by about an order of magnitude when accounting for them.

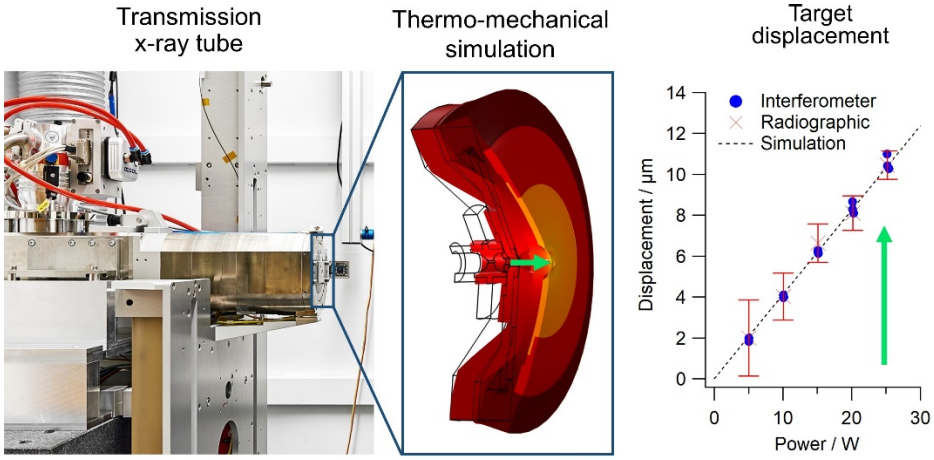

Figure 5: Effect of thermal transmission target deformation at different effective power levels.

At PTB the effect of the spectra dependent penetration depth of X-rays into the scintillator of the detector has been studied. Due to the penetration depth the position of the effective detector plane changes in dependence of the X-ray spectrum which in turn varies during a CT scan because of beam hardening effects in the scanned object. In cone-beam CT this effect leads to spectra dependence of the geometric magnification (Figure 6). The impact on the magnification of 2D radiographs was observed to be in the order of 10^{-4} - 10^{-5}. A correction method based on radial redistribution of intensities has been developed and validated. To determine the parameters for the penetration depth correction method a tool for simulation of the penetration depth was developed as well, which uses an analytical model to decrease computation time. The analytical model was verified to yield accurate results by comparison with Monte-Carlo simulations. On 2D radiographs of hole grids the penetration depth correction reduced the error of magnification by a factor of five. To verify the influence on 3D data, CT scans of a hole plate were analysed, however, the results remained inconclusive. The observed error of magnification did not show the behaviour expected from the penetration depth effect and, hence, the correction method could not be verified to significantly reduce the errors of dimensional measurements.

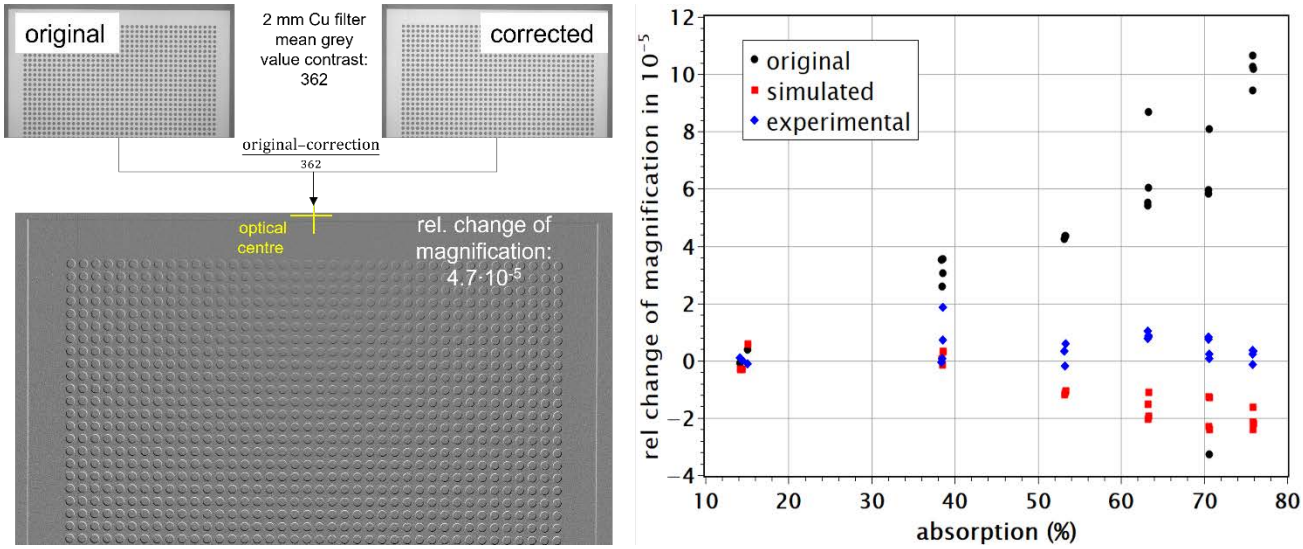

Figure 6: Energy dependent detector effects. Left: Difference images between corrected and uncorrected images of a grid-like test chart made of Cu. Right: Plots of the relative scale error observed at 150 kV in dependence of the absorption $(I-I_0)/I$ for the original data and after correction using parameters gained from experimental data and from simulation of the PD.

Compensation of CT geometry errors

The developed methodologies enabled geometry corrections with accuracies to below 1 µm and improved measurement uncertainty estimates. To account for non-ideal CT scan trajectories during reconstruction, a standardised CT geometry file format (openCTJSON) was developed in Objective 4 for the reconstruction algorithms in aRTist and VG Studio MAX (BAM, VG). Furthermore, interfaces to reconstruction algorithms accepting non-ideal trajectories, e.g., CERA, were put in place (BAM, METAS, Yxlon).

The positioning systems of two commercial and one research CT system were characterised using interferometry, electronic levels, and tactile probes at VTT, FSB, and METAS (Figure 7). Uncorrected, these deviations would lead to substantially deteriorated accuracies in dimensional measurements. Accounting for typical mechanical rotary axis errors increased the CT data accuracy about fourfold (Figure 8).

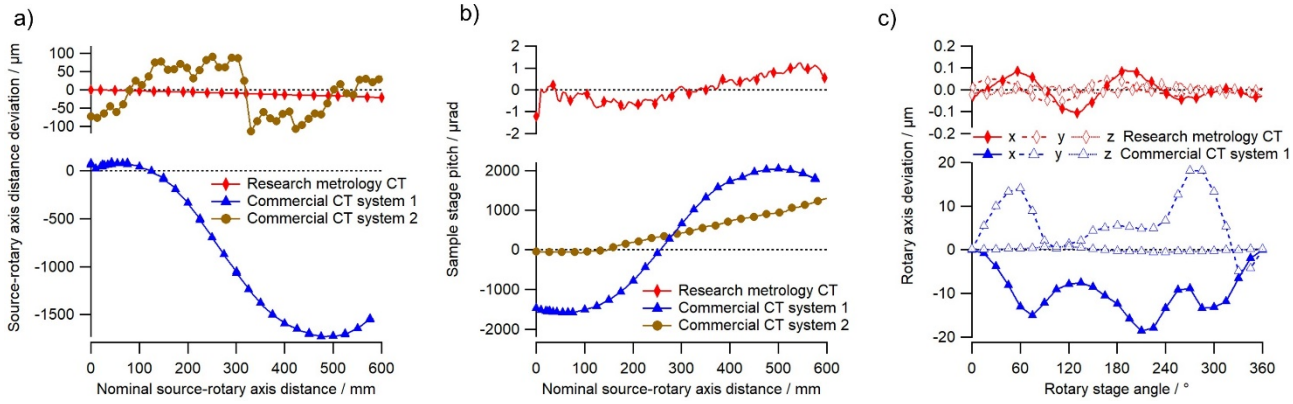

Figure 7: Stage error motions of three CT systems: Position accuracy along the magnification axis (a), pitch error of the rotary state (b) and rotary axis error motions (c).

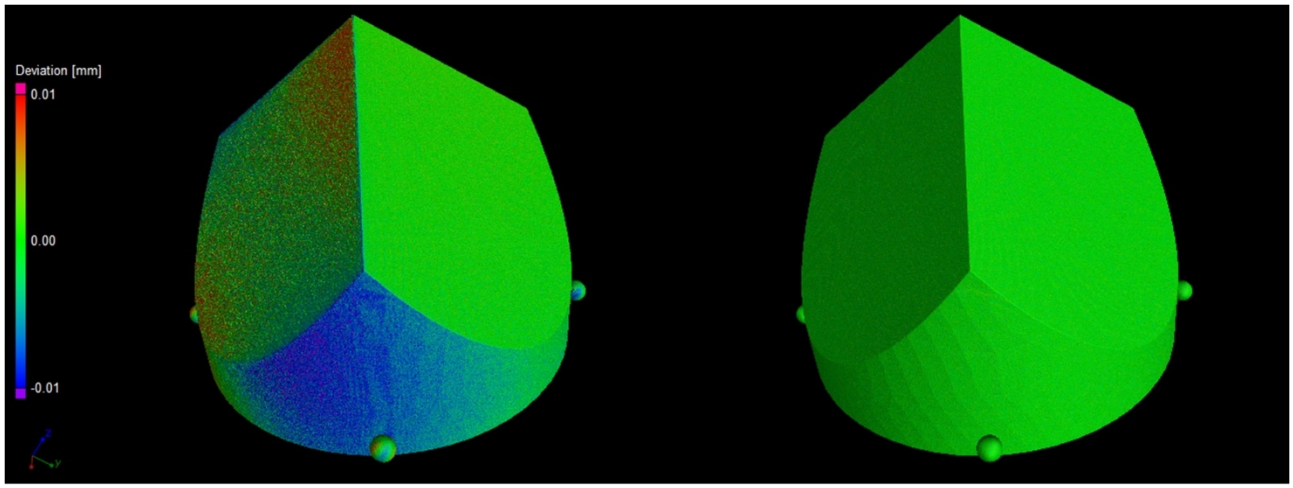

Figure 8: Simulation of the effect of a non-ideal rotary axis without (left) and with compensation (right) during reconstruction.

At METAS, an *in situ* metrology system, consisting of interferometers and laser straightness sensors, was developed (Figure 9). It continuously monitors the CT geometry with micrometre accuracy. Accounting for the drift in source-rotary axis distance at high magnifications (~100×) during reconstruction, reduced the standard deviation of sphere-to-sphere distances about twofold. Compensating the geometry between the radiographic CT geometry calibration procedure and the actual CT scan, improved the scale error of high-magnification scans by about an order of magnitude and resulted in reproducible standard deviations of sphere-to-sphere distances below 50 nm (Figure 9).

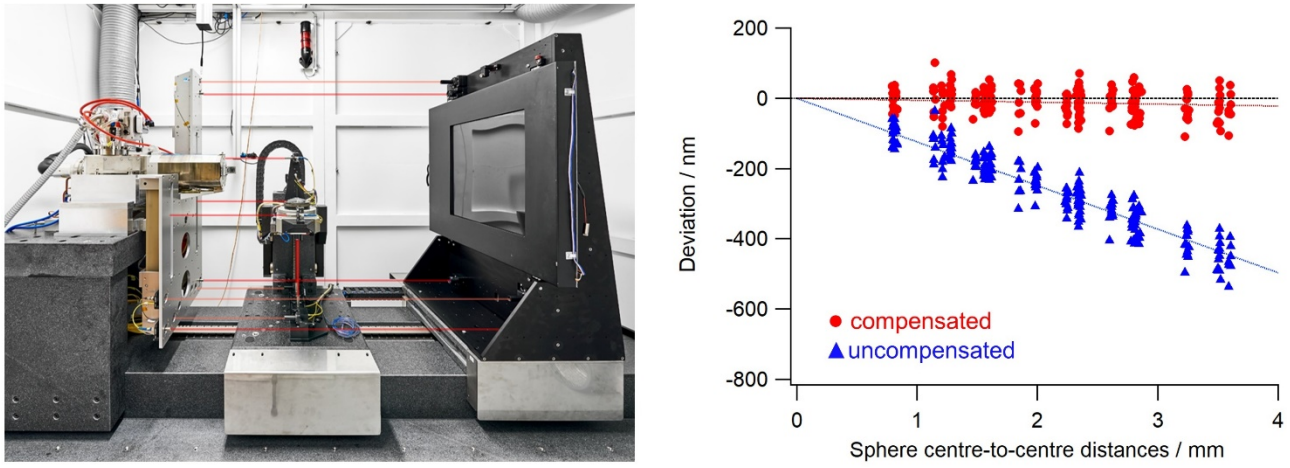

Figure 9: In situ metrology system on a dimensional CT and resulting improvement in accuracy of sphere-to-sphere distances.

Objective 1 was achieved and represents a fundamental contribution to substantially improve the accuracy of dimensional CT and to establish traceability. New reference standards and traceable calibration methods were developed to determine CT geometry with a higher accuracy and more efficiency. We carried out comprehensive characterisations of the temperature behaviour of different CT systems. The results were implemented into correction models and best practices. X-ray source and detector specific effects were investigated. Accounting for the movement of the X-ray tube was critical to achieve accurate measurements in high-resolution CT data. Energy-dependent detector effects were identified. Even though, their correction did not yet lead to conclusive results, it is important to incorporate them in the measurement uncertainty estimation. A unique *in situ* metrology system was developed to continuously measure the CT geometry. Besides enabling different influence factors to be studied, it also allows drift during CT scans to be corrected and, thus, achieve lower measurement uncertainties. Further, repeatable geometry errors, originating from the positioning systems, were mapped. Incorporating the geometry deviations in the reconstruction led to substantially more accurate CT measurement. The findings of Objective 1 enabled three National Metrology Institutes to provide new CT-calibration services.

Objective 2:

To develop improved and traceable methods for dimensional CT measurements with a focus on measurements of sculptured / freeform surfaces, roughness, and multi-material effects including supplementary material characterisation.

Objective 2 consists of three goals for dimensional CT measurements:

1) Develop improved, traceable methods for sculptured / freeform surfaces
2) Develop methods for surface or roughness characterisation
3) Develop methods for multi-material effects and material characterisation

Freeform CT

PTB conducted a study with additional data from DTI, Messtronik (collaborator), Werth and Zeiss, aimed at investigating three key aspects of freeform dimensional CT: freeform evaluation strategies, their traceability and registration of the CT volume. The hyperbolic paraboloid (HP) (Figure 10) was selected as a test object. The freeform surface follows a relatively simple mathematical equation, $z = A(x + B)(y + C) + D$, with the shape defined by the model parameters A (curvature) and B, C, D (offsets along orthogonal axes). The two versions of the part include reference spheres or calottes and were made from titanium (HPT) or a polymer (HPP) with a comparatively low absorption coefficient. DTI, Messtronik (collaborator), PTB, Werth and Zeiss scanned the two parts to provide CT data. PTB also carried out tactile reference measurements. The freeform surface was sampled in a regular point grid (a “CT grid” or “reference grid”, for the tactile measurement). Three spheres or calottes were also measured and used as registration features for a 3-2-1 registration of the measurement volume or tactile point cloud, and for scale corrections. Most datasets included repeat measurements, which were averaged together.

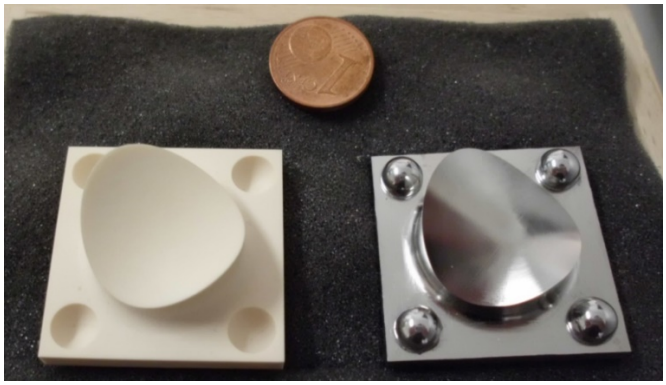

Figure 10: The hyperbolic paraboloid freeforms (courtesy of CMI [1, 2]).

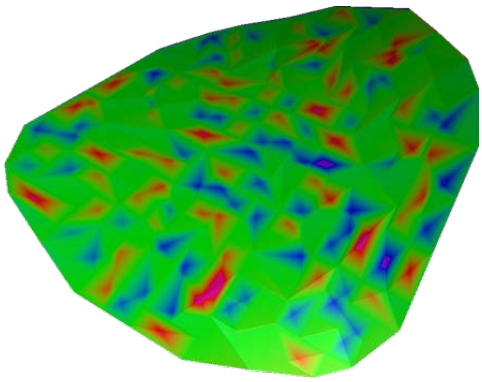

Figure 11: Nominal-actual comparison example.

The impact and robustness of object registration was investigated by running nominal-actual comparisons (NA) between a CT grid and the reference grid. The reference grid was always registered (3-2-1) based on the spheres. The CT grid was either 3-2-1 registered or best-fit registered, at two different quality settings, against the reference grid. The same procedure was repeated after applying an image deconvolution, developed as part of objective 4, to the CT volume and extracting the new CT grid.

The NA compares the surface meshes generated from the grid data and creates a colour-coded map to indicate the deviations of the CT from the reference surface. (Figure 11) The deviation map and distribution varied significantly depending on which registration method was used. This is a problem because usually, this type of result is used to check tolerances or even to guide remedial action for an out-of-tolerance part. As all results disagree, one cannot tell which, if any, is the correct or most accurate. After applying the image correction, however, the NA yielded the same outcome with each registration. Best fit is somewhat risky to use, as it may be less robust than feature-based registrations, and may alter the measurement results, particularly when an NA is used. Here, the study showed that best fit can obtain the same results as a 3-2-1 registration once the CT data quality has been improved by additional post-processing. This is particularly important for freeforms, since industrial freeform workpieces may not include any suitable registration features.

Measurement evaluation strategies are important because of the limitations a freeform may impose. This particular freeform can be modelled precisely. Often, freeforms can only be modelled or approximated in part by generic models such as splines, which are difficult to parametrise. The case study looked at three strategies to account for this: First, the model-based evaluation, using a least-squares fit and the equation to determine the model parameters A-D from the grid data, which are then used for comparisons. Second, point-based comparison, where each grid point is considered individually, looking at the z-shift (height change) relative to the reference (x, y are always constant). This represents the worst-case scenario, where no modelling is possible. Third, an intermediate approach using small surface patches. A patch is centred on the grid point, but includes the surrounding surface points, readily available from the CT scan. The patch centroid is compared to the tactile reference point. This reduces noise, avoids outliers and the centroid is still comparable to a sparse reference dataset. The normalised error criterion E_N from ISO17043 was used to confirm whether CT and reference values agreed. The normalised error considers the difference between two results as well as their associated uncertainties, estimates of which were provided by the participating partners (DTI, Messtronik, PTB, Werth, Zeiss).

The results show that all three strategies are viable, provided proper corrections have been applied to the CT data or volume. Two correction types were tested on some of the datasets. The most important is the scale correction, which tries to correct the voxel size of a CT volume.

The first method was a substitution measurement using the 2D hole foil developed by PTB. The calibrated foil was measured after the CT scan and used to accurately determine the voxel size at the object position. This approach was developed in Objective 1. The alternative was an internal standard, that is, a reference feature that is already part of the object to be measured. Instead of a “calibration scan”, the internal method relies on a separate measurement system. In this case, the reference spheres provided the reference features and the tactile CMM the reference value. The distance between spheres or sphere diameters were both tested. The voxel size was adjusted so that the measured average sphere distance or sphere diameter agreed with the tactile results. Both the 2D substitution and the sphere distance corrections worked very well, improving the measurement results in all cases. For example, the substitution reduced the failure rate of individual points from 82 % to 17.2 %; where the failure rate is the number of grid points that do not agree with their corresponding reference points (per E_N). (It should be noted that the patch strategy did not perform significantly better than the single point strategy). The sphere diameter failed with the HPP, which uses empty calottes whose shape is not of particularly high quality. This affected the sphere results, leading to a wrong scale correction. The HPT, by contrast, has high quality steel spheres fitted and scale correction worked well with either distances or diameters. This shows that reference features need to be chosen carefully.

The second correction was the image correction already used for registration testing. This yielded promising improvements with the HPT but was less effective with the HPP. The image deconvolution (see Objective 4) is better suited for strongly absorbing materials.

An effective scale correction is the most important factor in a successful and accurate freeform measurement. On top of the improved results, it establishes a link to the traceability chain, either through a calibrated reference body (substitute) or a calibrated secondary measurement system (internal standard).

<u>Calibration of XCT for additively manufactured surface texture evaluation</u>

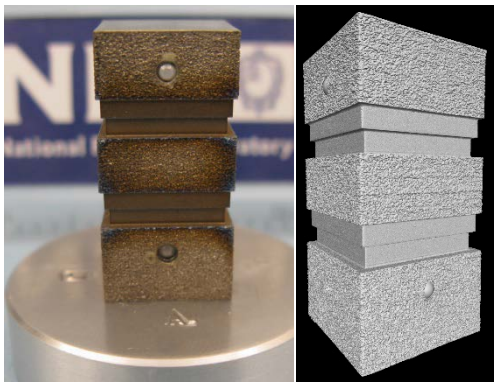

Figure 12: A prototype of NPL’s 3DRS measurement standard and an XCT image.

X-ray computed tomography (XCT) has been increasingly used for the inspection of additively manufactured (AM) components. However, calibration of XCT for surface texture evaluation has not been established. The project established a simple and effective way to provide XCT surface texture measuring traceability for AM surfaces via a profile method, where the choice of analysis has been mostly driven by the industrial need for simple, traditional roughness measurement traceability

In this project, NPL, PTB, BAM, DTI, FSB, LNE, METAS, VTT, CEA, EMPA, FAU, UBATH, UNOTT, UoS, Bosch, LEGO, NovoNordisk, Werth, Yxlon and Zeiss have explored various reference samples to calibrate XCT for surface texture evaluation, and NPL’s prototype 3D Roughness Sample (3DRS, see Figure 12) has been selected for this purpose. The 3DRS was manufactured by electron beam melting, a popular AM technique.

The design of the reference sample accommodates three distinct sets of features: spheres, one-sided steps (ST), and surface texture features. The sample has four faces with different *Ra* parameters, taking values between 10 µm and 40 µm, when filtered in accordance with ISO 3274.

To establish the traceable measurements, the project focused on the calibration of XCT for 2D profile evaluation. Measurement protocols have been established for both XCT and the reference instrument (a profile contact stylus (CS) instrument).

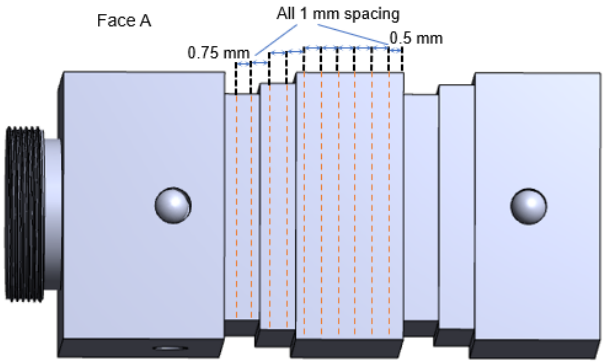

Figure 13: Measurement locations of the surface texture features.

Repeat measurements were conducted using XCT, considering measurement reproducibility. The data were then reconstructed into volumes and surfaces were extracted. Finally, profiles were extracted from the surfaces for analysis.

The project has investigated the suitability of different λ_S and λc filters. The λ_S filter defines the intersection between the roughness and shorter wavelength components. It has been observed from the results that using either 8 µm or 80 µm cut-offs bears no impact on the 3DRS sample's roughness profiles, which confirms that the dominant surface texture components have a spatial wavelength larger than 80 µm.

The λ_C filter defines the intersection between the roughness and waviness components, and its cut-off value is dependent on the value of *Ra*. In the project, both 2.5 mm and 0.8 mm values for λ_C were studied. The λ_C cut-off of 0.8 mm appears to filter some of the waviness components of the XCT errors that influence the overall shape of the measured component. A 2.5 mm filter appeared to preserve more surface information, but there is a lack of guidance to define surface waviness and roughness.

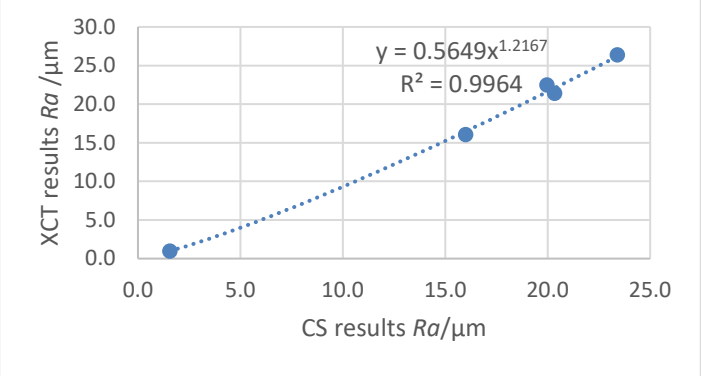

Figure 14: Relationship between XCT and CS data with the filter of λs = 80 µm, λc = 2.5 mm.

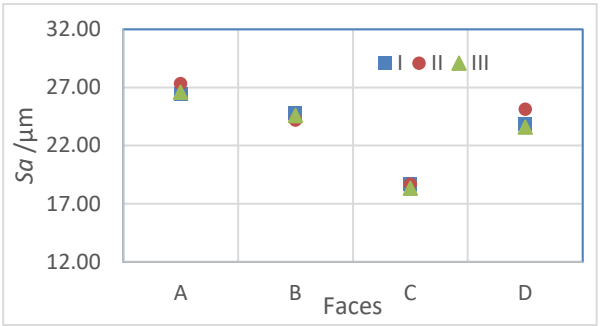

Figure 15: Comparison between three XCT instruments, with L-filter of 2.5 mm and S-filter of 0.08 mm.

The uncertainty evaluation of surface texture using a calibrated reference standard follows the general guideline defined in GUM. In the case of XCT surface roughness measurement, traceability was established via an AM roughness comparison specimen, and the uncertainty has been evaluated.

Further study has been conducted in the project to include three different XCT systems to investigate the behaviour of different instruments. The data has been processed and the surface texture evaluation of areal data followed the guidance in the international standards ISO 25178-3 and ISO 25178-2. It was concluded that areal evaluation could be conducted using XCT and produce repeatable results with small measurement uncertainty, as it is well known that the areal method provides superior statistical relevance compared to profile methods. It is also worth noting how much the AM surface uniformity affects the profile measurements' reproducibility. There is a large gap in the current additive manufacturing technology's ability to produce AM reference artefacts to the expected level of surface texture uniformity in a cost-effective manner. However, areal characterisation can overcome this issue. The other avenue to further improve uncertainty evaluation is to increase the number of repeat measurements.

With the well-established procedure and reference sample, the calibration process can be automated, which reduces the burden for operators to implement more measurements and data analyses.

Case studies in XCT surface texture measurement

Case study applications of the methods developed during this objective were performed, including the following samples: NovoNordisk – Internal surface roughness in small bore needles; LEGO – surface texture of small polymer parts; and University of Nottingham (UNOTT) – additively manufactured internal channels.

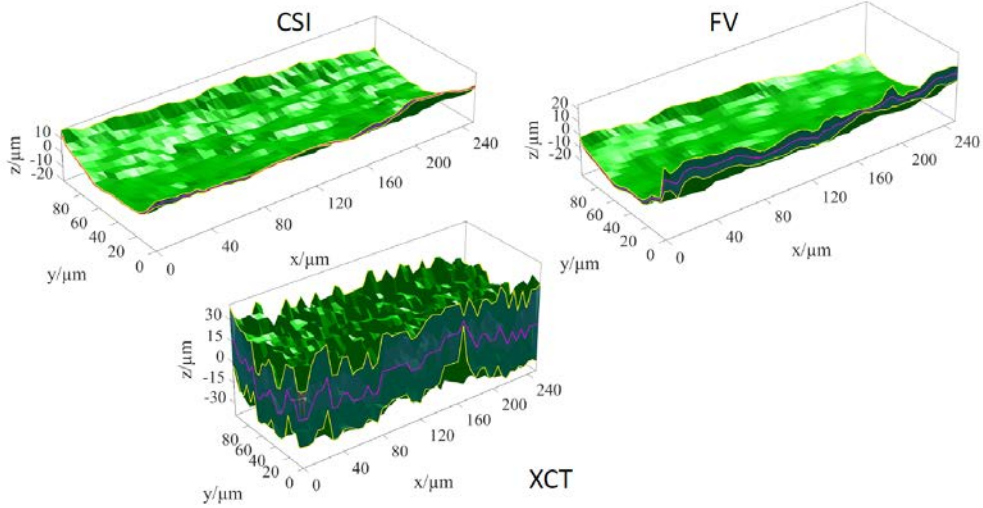

Figure 16: Direct topography comparison between three coherence scanning interferometry (CSI), focus variation (FV) and XCT instruments. Mean surfaces, with upper and lower bounds at 95 % confidence for a NovoNordisk needle.

Multi-materials and material characterisation

Practical CT measurements are frequently confronted with multi-material workpieces, i.e., parts made of more than one material with different absorption coefficients. This may introduce metal artefacts. A strongly absorbing component may lead to beam hardening and other effects creating streak artefacts (see Figure 17). A common problem, for which the medical field has developed correction methods, some of which PTB implemented and tested with support from Bosch and Yxlon for a dimensional – quantitative – measurement. Commercial solutions are also available and were tested as well. The metal artefact reduction techniques show great qualitative improvements to an affected volume. However, while quantitative measurements are also improved, the remaining deviations are still significant, with reductions from hundreds down to several tens of micrometres.

Another issue is the multi-material surface determination, i.e., the location boundary between two materials. This can be difficult for materials with similar absorption coefficient as, to a CT scanner, they are virtually indistinguishable. This was tested, both experimentally and in simulations with PTB's multi-material standard (see Figure 18). One- and two-step surface determination algorithms were compared for their dimensional performance, with the latter producing significantly better results. The trials also established a boundary, a minimum difference between material absorption coefficients, above which one-step algorithms are generally safe to use.

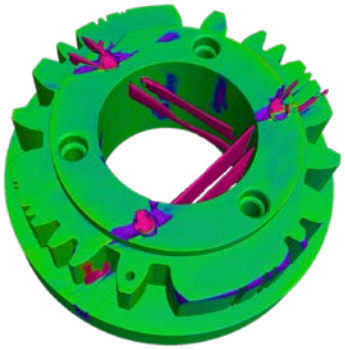

Figure 17: Metal artefacts from steel pins in a titanium part.

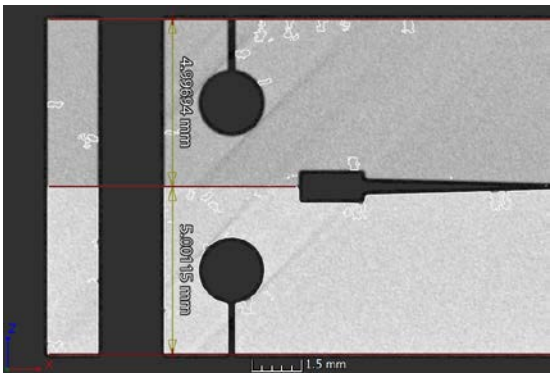

Figure 18: Tomogram of the multi-material standard. Phantom surfaces appear in the material blocks as the surface determination struggles with two very similar materials.

Dual-energy materials characterisation and material-dependent X-ray phase contrast

Synchrotron CT was used by BAM for materials characterisation and to evaluate the multi-material effects on measurement uncertainty. Two calibrated tetrahedrons of four spheres from ruby and silicon nitride or steel were investigated. The multi-material objects were measured at BAMline at the BESSY II synchrotron source at different object-detector distances and energies.

The dual-energy materials characterisation aims to decompose the linear attenuation coefficient measured with XCT into the material features of density and effective atomic number. By measuring at two different energies and solving a system of linear equations the material features are determined for every voxel of the CT data (see Figure 19). The dual-energy analysis was calibrated with the theoretical values of ruby. For steel, the material features could be accurately determined with a relative error of less than 2 %. The dark inhomogeneities in the CT data of the steel sphere vanished in the image of the atomic number Z (top, right) while still present in the image of the density ρ (bottom, right). This can be explained by the fact that different phases in steel may have different electron density, but still the same elemental composition. For silicon nitride, where the XCT contrast to ruby is marginal, it was not possible to reveal the correct material features, but the material discrimination became possible after the dual-energy analysis.

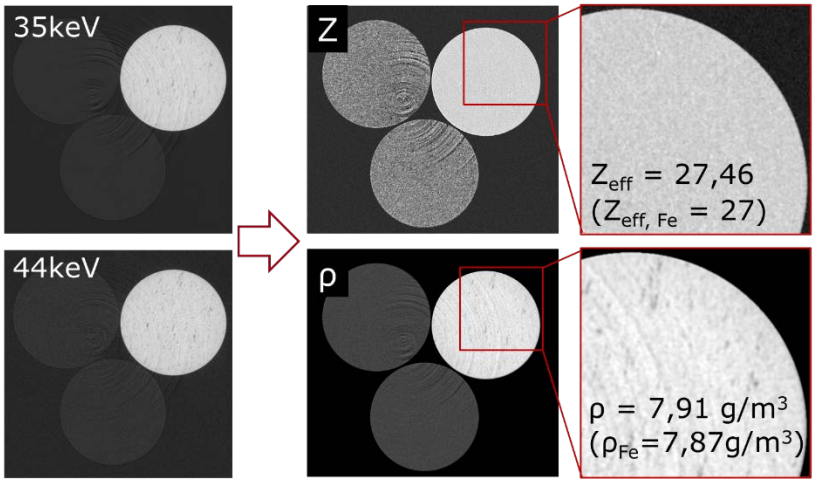

Figure 19: Synchrotron CT slices of a multi-material (ruby and steel) tetrahedron measured at two energies and resulting dual-energy analysis of effective atomic number and density.

The X-ray phase contrast effect, which is most prevalent at high resolution CT scans, originates from the refraction of the X-rays and leads to an enhancement of the edges and this influences the surface determination and dimensional measurements. Synchrotron CT allows the influence of the material-dependent phase contrast on dimensional measurements to be studied in isolation due to its parallel beam geometry and the highly coherent X-ray source. An initial (reference) CT measurement was carried out at the smallest possible object-detector distance of Z = 3 mm to get minimal phase contrast on the reconstructed data. To follow the evolution of the refraction driven phase contrast, two additional scans were performed at increased object-detector distance of Z = 15 mm and Z = 45 mm. Two algorithms, Paganin's phase retrieval and

Bronnikov's phase retrieval, for correction of the phase contrast were applied to the data. Both algorithms successfully removed the phase contrast on the datasets. The uncertainty evaluation revealed the significant increase of the error of diameter determination at higher distances for the uncorrected datasets. A material dependence could not be observed. In the case of the sphere diameters, the Paganin's algorithm led to a significant reduction of the deviation for Z = 15 mm and a moderate reduction for Z = 45 mm. Bronnikov's algorithms better preserve the image sharpness but could not improve the measurement uncertainty.

Summarising the results of the work on objective 2, traceability for freeform measurements was successfully established by two methods. Essential corrections were identified for the purposes of traceability and quantitative measurement – scale corrections – and robust, repeatable freeform artefact registration – image deconvolution. Roughness reference standards suitable for CT were developed and successfully tested with 2D-profile and 3D areal evaluation methods. Boundary conditions were established for surface determination within multi-material CT scans. Dual energy scans were also investigated. A quantitative evaluation of existing metal artefact corrections addressed this type of artefact in the context of metrological/industrial CT scans. Material characterisation was also addressed by an in-depth study of phase contrast corrections and their effects on dimensions. All tasks in Objective 2 were achieved except the competition of the investigations on the influence of X-ray refraction and phase retrieval algorithms on dimensional measurements with synchrotron X-ray computed tomography.

Objective 3

To develop fast CT methods for inline applications based on improved evaluation of noisy, sparse, few, or limited angle X-ray projections, and reconstruction methods. This was undertaken using a reduced number of projections from well-known directions and include enhanced post-processing.

Framework for testing reconstruction algorithms

XCT is increasingly used as a non-destructive evaluation technique in industry. However, the cost of measurement time and data storage hampers the adoption of the technique in production lines. Filtered back-projection (FBP, in cone beam CT FDK) based reconstruction algorithms are analytical algorithms that are still widely used due to their efficiency in reconstruction. However, FBP based algorithms require a large number of projection images to fulfil the Shannon sampling theorem to eliminate image artefacts. This is one of the factors limiting the speed of measurements. The project has reviewed the latest development of the reconstruction algorithms for the purposes of handling a limited number of projections, limited angled data and also scans with short X-ray exposure time.

In the project, several advanced algorithms have been established. Total variation (TV) based algorithms show great performances, especially when dealing with limited projection data if they were run with suitable hyperparameters. Improvements based on an algorithm originally introduced by Freund and Sapphire in 1997 and an implanted virtual reference has been established to improve hyper-parameter selection for TV-based algorithms. Additionally, a genetic algorithm based hyperparameter selection in a TV based algorithm was developed. A fast version of the TV constrained reconstruction algorithm FISTA and a deep learning algorithm using convolution neural network (CNN) and based on freely available platform TensorFlow (used a U-net), have been developed.

To evaluate these reconstruction algorithms, reference samples have been selected by NPL, PTB, BAM, CEA, UBATH, UoS, Yxlon, Zeiss and evaluation frameworks have been developed. The three reference samples selected were: NPL's AM reference sample, PTB's hole plate, and EMPA's step cylinder, as shown in Figure 20. Both simulation data and experimental data have been used. The simulation was conducted using aRTist software. Experimental data were conducted using commercial XCT systems selected across the consortium to measure physical samples.

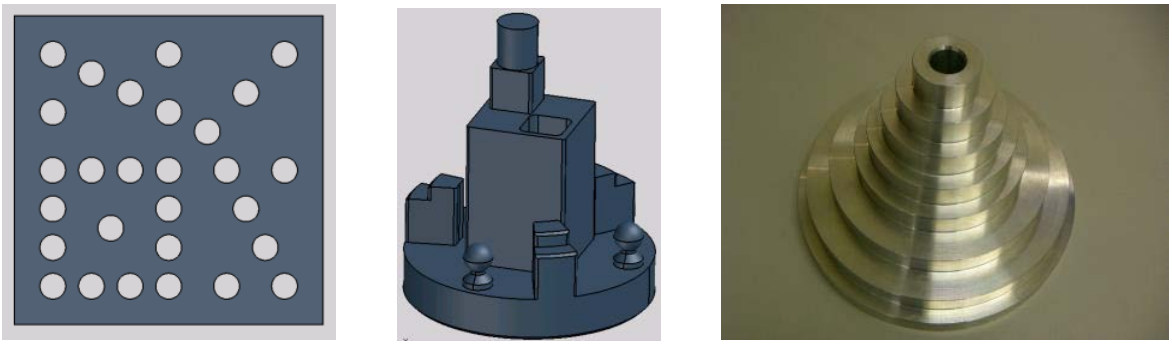

Figure 20: Reference samples selected for evaluation. Left, PTB's hole plate. Middle, NPL's AM reference sample. Right, EMPA's step cylinder.

A benchmark strategy of the performance evaluation of various reconstruction algorithms has been established and evaluations were conducted based on the algorithms available in the Tomographic Iterative GPU-based Reconstruction (TIGRE) toolbox. The benchmarking criteria include both image quality metrics and dimensional evaluation metrics, as shown in Figure 21. The investigation focused on the performance of the reconstruction algorithms with measurements with limited projections, limited angular range and significantly reduced exposure times to facilitate faster CT acquisitions. A diagram of the process is presented in Figure 21.

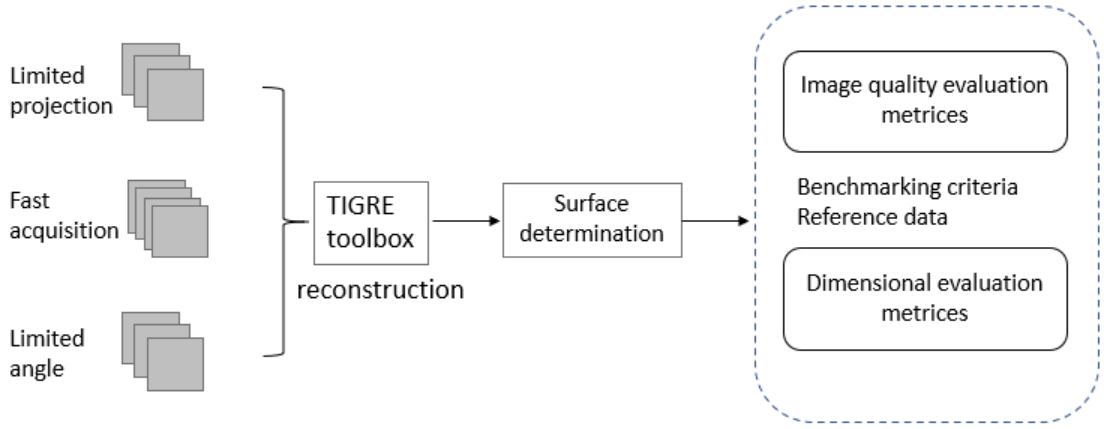

Figure 21: Framework for the evaluation of reconstruction algorithms.

Development of a metrology software toolkit

The TIGRE tomographic reconstruction software, originally developed by the University of Bath (UBATH) and CERN, has been further developed in the project by the University of Southampton (UoS), to overcome previous size and speed limitations for iterative algorithms. As the datasets generated in modern XCT far exceed the memory available internally in commercial parallel computing hardware (i.e. the graphical processing units (GPUs) required for efficient computation), efficient data splitting and transfer protocols needed to be developed. The new software is now no longer bounded by available GPU memory and instead has the potential to allow the reconstruction of arbitrarily large volumes (now mainly limited by the computing system's RAM). The enhanced software toolkit also allows the efficient utilisation of several GPUs in parallel. A new implementation of the FISTA (Fast Iterative Shrinkage/Thresholding Algorithm) was also added to the toolbox to allow fast and efficient reconstruction using a Total Variation constraint.

Characterisation of reconstruction algorithms

- Evaluation of reconstruction algorithms with a limited number of projection images.
- The Ordered-Subset Adaptive Steepest Descent Projection Onto Convex Set (OS-ASD-POCS) algorithm has been evaluated in contrast to Ordered-Subset Simultaneous Algebraic Reconstruction (OS-SART) and FDK in handling a significantly reduced number of projection images (from 3142 to 60 projection

images) for reconstruction, which allows a reduction of measurement time from fifty-two minutes to one minute for a typical industrial XCT system. It also enables a reduction of data size proportionally. An example of comparison is shown in Figure 22.

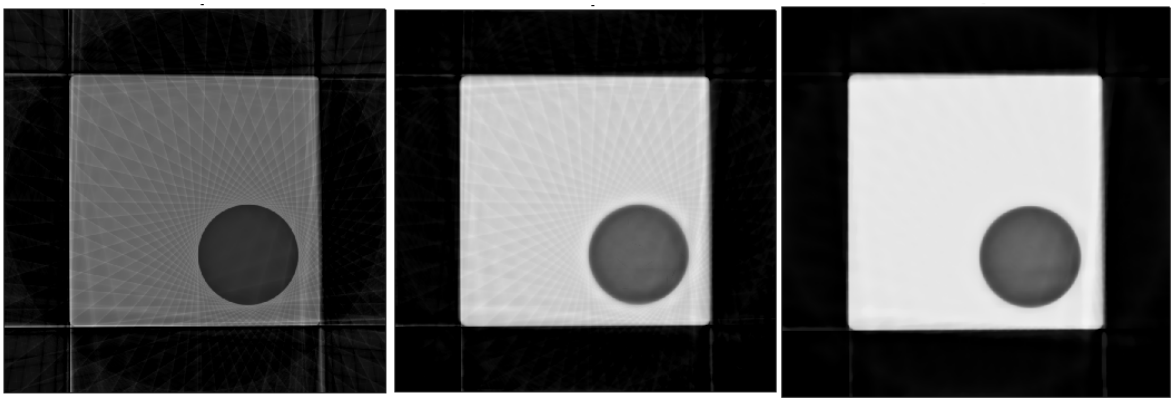

Figure 22: Reconstruction based on 60 projection images using different reconstruction algorithms. Left. FDK algorithm, Middle. OS-SART algorithm with 60 iterations. Right. OS-ASD-POCS algorithm with 60 iterations.

A test strategy including both quantitative and qualitative test metrics was considered to evaluate the effectiveness of the reconstruction algorithm. The qualitative evaluation includes both the signal to noise ratio, the contrast to noise ratio, etc. The quantitative evaluation was established using reference samples with different internal and external geometries. Simulation data were used in the assessment considering various influence factors, including beam hardening and noise.

The results demonstrated the possibility of using advanced reconstruction algorithms in handling XCT measurements with a significantly limited number of projection images for dimensional measurements. This work laid down the foundation of conducting fast XCT measurements without the need for instrument alteration or enhancement. Although the reconstruction time required is still considerable, various possibilities to improve this have been investigated in the project.

- Evaluation of reconstruction algorithms with limited angles of projection images.
- Two iterative algorithms, the Conjugate Gradient Least squares (CGLS) and Simultaneous Iterative Reconstructive Technique (SIRT) in addition to the FDK algorithm, were evaluated for data with limited angle trajectories. Different under-samplings of the complete set of projections have been carried out to test the algorithm with reduced projections and/or limited angle trajectory (270°). In terms of time, the iterative algorithms were taking considerably higher time. However, the CGLS algorithm was performing better when looking at the Root-Mean-Squared Errors (RMSE) and L2 error results. On further comparison of the post-reconstruction analyses, it can be concluded that the SIRT resulted in a very bad reconstruction with poor contrast, which eventually leads to poor definition of the features (holes). FDK and CGLS produced very comparable results. However, FDK-based results are affected by limited projection and a limited angular range approach, unlike CGLS. Therefore, the CGLS iterative algorithm can be preferred over FDK when there is a small number of projections and/or partial angle datasets are available, which could then justify its longer execution time. It is worth noticing that the TV based algorithms can provide sharper images due to its sparsity enhanced performance. CGLS and algebraic reconstruction technique (ART) type image reconstruction tend to produce images that are more blurred in the interface between materials.

- Evaluation of reconstruction algorithms with fast acquisition.

The project also characterised the performance of different reconstruction algorithms as a function of observation and reconstruction noise. An aluminium step cylinder (see Figure 23) as well as an aluminium hole plate were scanned using a slow, low noise scan and a fast (short exposure), high noise scan for comparison. The results were also compared to a scan with a limited number of projection images.

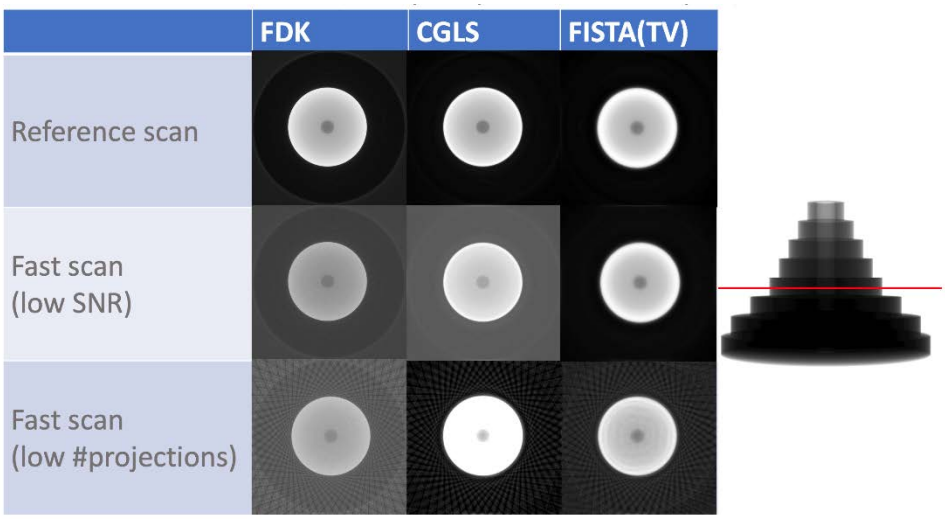

Figure 23: Cross-section comparison of images reconstructed using FDK, CGLS and FISTA(TV).

Figure 23 illustrates images reconstructed using the FDK algorithm, the conjugate gradient least squares algorithm (CGLS) and a total variation regularised least square reconstruction using the FISTA (TV).

The results indicate that advanced algorithms, such as the iterative CGLS and FISTA algorithms do provide useful dimensional measurements in cases where traditional methods no longer work, though at the cost of the significantly increased reconstruction times required. However, CGLS and FISTA were both found to bias surface estimates, often leading to smaller internal and larger external hole diameter measurements. FISTA(TV) also required careful parameter tuning and was found to often lead to dimensional measurements with an increased measurement uncertainty.

In order to characterise the suitability of the modern CT reconstruction algorithms implemented in Objective 3 for use in image reconstruction software, the project investigated the influence of reconstruction algorithms on quality vs. time requirements. CGLS, MLEM, SIRT, OS-SART, OS-SART-TV, and FISTA were evaluated, with FDK serving as the baseline.

While having higher computational demands and generally increasing reconstruction times when compared to FDK, the investigated iterative reconstruction methods can provide benefits for Fast CT. This primarily applies when a reduced number of projections is used, simultaneously decreasing scan and reconstruction times. Iterative reconstructions were also found to provide benefits for limited-angle scans. In particular OS-SART and OS-SART-TV were found to generally converge fastest to a sufficiently good result. With dimensional evaluation as the primary goal, initialisation of the reconstruction volume with the FDK result before applying iterative methods allows for much faster convergence than the default configuration and can be recommended. Even so, the iterative reconstruction algorithms provided no significant benefit over FDK for the measurement of macroscopic features in most of the evaluated scenarios. Their advantages become more relevant with very low projection counts (in the order of 60), missing or unevenly distributed projections, or very noisy data (SNR less than approximately 10).

.

State-of-the-art instruments for fast CT

The project has reviewed the definition of “fast CT”. Based on market survey, scan times of a few minutes or less are considered as fast CT. A survey was conducted, asking market players to provide a CT system or model series currently being marketed for general fast CT applications.

The presented fast CT systems generally follow the typical industrial CT design, with a stationary source and detector arranged around an adjustable rotary stage inside a stand-alone cabinet. All use reflection X-ray tubes with voltages in excess of 225 kV and powers of up to 1800 W. Detectors are flat-panel detectors (FPD) with varying specifications. Most systems are designed to accept larger samples (300 mm × 300 mm or larger) with a weight of 30 kg or more; only one was limited to smaller samples (200 mm × 200 mm, 2-4 kg). Unfortunately, performance metrics (e.g., resolution) were either unavailable or provided in very different formats, making a direct comparison impossible. In any case, such metrics are application-dependent and change with the current operating conditions of the CT system.

The typical acquisition times achievable with the presented fast CT systems are two minutes or less, for a general “fast CT” or inline application. A round-robin style comparison was beyond the scope of this activity. One manufacturer provided a more detailed breakdown of measurements of different, small parts made from plastics or rubber. For these, the reported accuracy was several tens of microns for scans taking up to two minutes. A scan for metrology and defect analysis of a large aluminum part took 30 minutes in total, illustrating how the task can affect the achievable speed. It is therefore very difficult to benchmark CT applications without running a controlled test of the systems involved.

Fast CT case study

The step cylinders, see Figure 24, were selected as test pieces for the fast CT case study. They include internal and external features – calottes, grooves and cylinders – from which a range of GD&T-type measurands can be derived. Because of the increasing step diameter (8 mm-28 mm) and the different available materials (ABS, Al, steel), the stepped cylinders neatly embody a difficulty scale for CT measurements. Unfortunately, the parts, which were also used for other activities, accumulated damage over time (e.g., cracking). Hence a quantitative evaluation of the study is difficult at best.

T 

Figure 24: Three step cylinders in different materials and their internal structure.

Three partners (Werth, YXLON, Zeiss) used commercial fast CT (cFCT) modes, implemented by the CT manufacturer in the control software. Any optimisation to reduce acquisition time is handled internally by the software. Scanning times decreased significantly, e.g., from 60 to 20 minutes, which is still much longer than in-line applications (~1 minute). The software did this by optimising exposure time, projection count or both. However, the speed-up did not have any impact on the data quality; quantitative measurements obtained from the same system with and without cFCT did not differ significantly.

Manually optimised fast CT acquisition (from Messtronik) was much faster (3 min - 8 min) as even lower projection counts or exposure times may be set but come with obvious losses in data quality. Noise particles in and around the artefacts impacted the surface determination and affected or even erased features, particularly those inside the workpieces. Identifiable measurands also differed significantly from reference values obtained from normal CT scans. However, the progressive damage to the parts may also have played a role in this.

Overall, the results show that cFCT appears to be an effective and straight-forward way for users to somewhat reduce measurement times without sacrificing quality. Faster scans are possible but require careful setup and

optimisation. Depending on the situation, a low-quality scan may still be sufficient to evaluate features of interest at an acceptable level of accuracy.

In summary, the project has successfully met the target set in the objective 3. Fast CT methods have been evaluated with consideration of noisy, sparse, few, or limited angle X-ray projections, and enhanced reconstruction methods have been developed. A comprehensive evaluation has been conducted with consideration of both qualitative and quantitative evaluation. Fast CT methods have also been tested using commercial CT to demonstrate feasibility.

Objective 4:

To develop traceable methods for uncertainty estimation using virtual CT models and Monte-Carlo simulations. Batch simulation and evaluation capacities was improved. The determination of accurate model parameters was necessary for a reliable uncertainty estimation and this was performed for different CTs and it was systematised. Corrections for several artefacts were developed. Uncertainty was estimated by Monte-Carlo based simulation and verified using the calibrated standards developed in WP1.

Software tools for virtual CT

With the availability of software packages which can provide nearly realistic synthetic radiographs, uncertainty estimation is, in principle, possible based on virtual CT models. Enhanced software tools are needed to commonly apply methodologies to perform an uncertainty estimation of CT, via simulation. Within the framework of this project BAM has extended the simulator aRTist with a GUI module dedicated to uncertainty estimations. Additionally, the detector model has been improved. EMPA has further developed the generic, Monte-Carlo simulation system based on the GEANT4 toolkit and has used it to assess the influence of the system and the measurement parameters.

The developed add-on module for aRTist (AdvanCT module) supports simulation-based uncertainty estimations by a graphical user interface to parameterise repeated virtual CT scans with parameter variations. Before using the AdvanCT module, the basic set-up of a CT scanner must be modelled in aRTist. This includes source and detector properties as well as the geometrical configuration including the measuring object. Based on the static set-up of the first projection (see Figure 25 left) the AdvanCT module (Figure 25 right) can be used for batch simulations considering scan trajectories and additional variations of exposure and geometry. These additional variations can be used to introduce the real-world deviations characterising a specific CT scanner into the virtual model, as it is needed for uncertainty estimation.

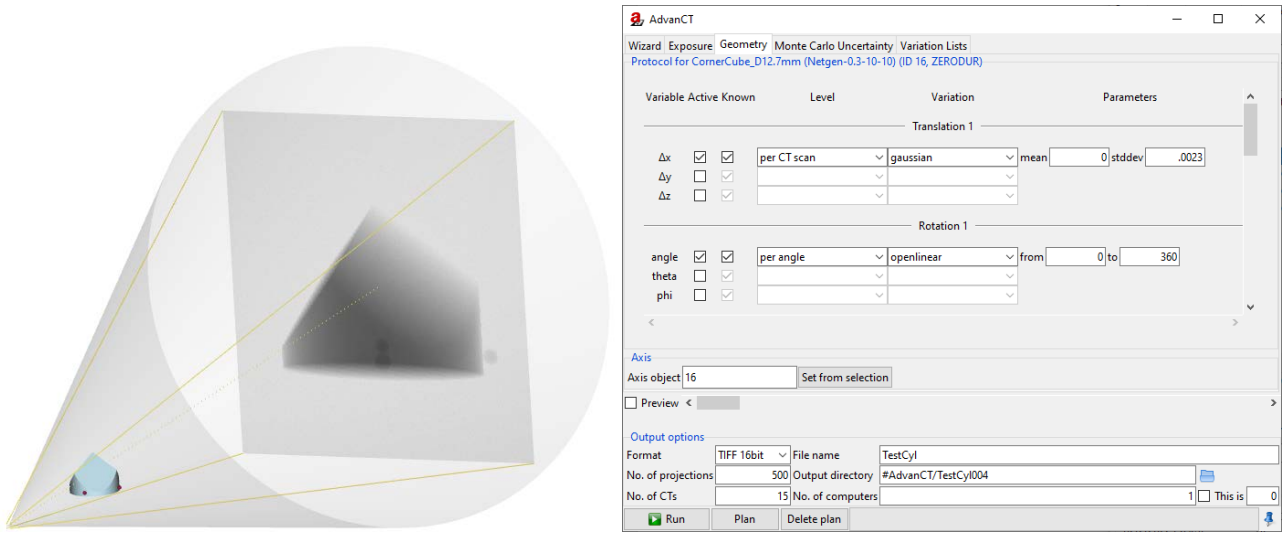

Figure 25: Virtual scene of simulator aRTist with METAS corner cube (left) and add-on module AdvanCT (right).

A variation can be described by a schedule of deviations for each projection of the batch simulation. For the definition of variation schedules there is a set of deterministic and random functions, e.g. linear or Gaussian variations. But it is also possible to read in a schedule from a table provided by an external file. Furthermore,

a schedule can be applied per projection or per scan, where in the latter case a parameter changes per scan, but not between the projections of the same scan. Special schedules are available for Monte Carlo uncertainty propagation providing quasi-random variations. These can be used on a per-projection basis to implement the quasi-Monte Carlo method for uncertainty propagation using low-discrepancy sequences on a per scan basis.

Variation schedules can be applied to alter exposure parameters, like tube voltage and current, and to change the geometrical configuration. Each geometrical element of the virtual scene including source and detector can be assigned by several variation schedules controlling its position, orientation, and size. This enables maximum geometrical freedom to model realistic deviations for uncertainty propagation at standard trajectories and makes it possible to simulate free-trajectory scans.

Virtual CT generates projection data that can be reconstructed just like real CT scans. In addition to the projection data the AdvanCT module generates configuration files to interface with reconstruction software. This interface provides for each projection an individual projection matrix. Each variation schedule configured at the AdvanCT module can be marked as “known”. In this case, a variation is considered by the projection matrix and is thus made known to the reconstruction software. The variations defining the scan trajectory need to be made known to the reconstruction software, in contrast to the deviations contributing to the measurement uncertainty. The interface has been tested with three reconstruction programs: CERA by Siemens Healthineers, VGSTUDIO by Volume Graphics, and clFDK by BAM. For the interface BAM and VG have developed the file format openCTJSON as an open communication standard between CT scanners and reconstruction software.

Since virtual CT generally requires a certain computational effort, batch simulations for uncertainty propagation may be quite time consuming. The time for a virtual scan with aRTist is highly configuration-dependent, but often takes longer than the real scan. To address the application-limiting factor of computing time, the AdvanCT module can be used to prepare batch simulations which can be distributed among several computers. This includes the use of Supercomputers, which has been tested at the high-performance computing cluster IRIDIS5 of UoS. Considerable preparation was necessary to run aRTist at IRIDIS5. First, a Linux version of aRTist has been created and tested, since aRTist was only available for the Windows platform. Then the unattended command-line execution has been configured as aRTist is generally controlled by a graphical user interface. Finally, scripts have been compiled to distribute the batch simulation jobs planned with the AdvanCT module by the scheduler at IRIDIS5.

EMPA developed a generic virtual CT software model based on the GEANT4 Monte Carlo simulation toolkit, which was developed at CERN. The generic model includes a simplified Detector, X-ray source and test samples. The construction of the geometry is implemented with Constructed Solid Geometry elements. For material definitions the GEANT4 material database is used. For the parametrisation of all major components of the generic CT simulation software a database model was designed and implemented in an embedded SQLite database. Free available GUI-Applications for managing SQLite-Databases allow the easy configuration of the runtime, physical, geometric, and material simulation parameters.

During the project, software tools for virtual CT have been further developed with respect to their application for simulation-based uncertainty estimation. This enables the creation of realistic models of XCT systems including deviations from the ideal geometry, the scheduling of batch executions for Monte-Carlo uncertainty propagation, and the provision of the necessary computer resources through distributed computing. With the successful integration of simulations into the dimensional XCT measurement process, the objective was fully achieved.

Determination of accurate model parameters

A simulation-based approach of estimating the uncertainty of a computed tomography (XCT) measurement requires a representative model of the XCT system including deviations from the ideal geometry. The virtual model needs to be integrated into the dimensional XCT processing chain. Here a systematic procedure has been explored by FAU, METAS, PTB, and YXLON with help of VG and Zeiss, to include geometrical deviations in virtual XCT models.

The cumulated surface distance (CSD) of the resulting surface deviation histograms compared to a CMM corrected STL model has been identified as a suitable parameter to qualitatively describe the similarity between simulated and measured data. Two experimental methods have been evaluated to integrate geometrical deviations into an aRTist simulation. An experimental approach iteratively estimates a reduced set of geometrical deviation parameters by minimising the CSD. The second approach determines a

condensed set of geometrical deviation parameters based on radiographically measured distributions. Both approaches have been individually tested on different XCT systems or workpieces. The radiographically measured approach was found to be in good agreement even for bi-directional feature uncertainties whereas the iteratively estimated approach revealed some directional dependencies.

With support from VG a full iterative automation has been achieved for one example but setting up a fully automated optimisation process is currently very difficult. Moreover, there are still deviations between virtual and real XCT systems, as there is usually an information deficit, especially regarding the source and detector model. Further research is needed towards a true digital twin.

Corrections for CT artefacts

X-ray CT results in volume data, where each volume element is determined by the material at the represented real-world position. Inherent to the measurement process, fluctuations might occur in the volume data at regions representing homogeneous material, here called CT artefacts. Relevant origins of such image forming artefacts are source and detector properties, the sample geometry, and deviations from the assumed scan trajectory.

A systematic overview of relevant origins of image forming artefacts identifying more than ten distinct types has been compiled by PTB. Some types are generally handled appropriately by the CT supplier's software. Two dominant static image artefacts have been treated by deconvolution: a corona artefact due to scattering apertures acting as a parasitic source, and visible light transport in the detector's scintillator (blooming, halo, scatter). The burn-in effect (gain-drift), a dynamic artefact, could be modelled and removed by a logarithmic correction of the accumulated irradiation dose on each detector pixel.

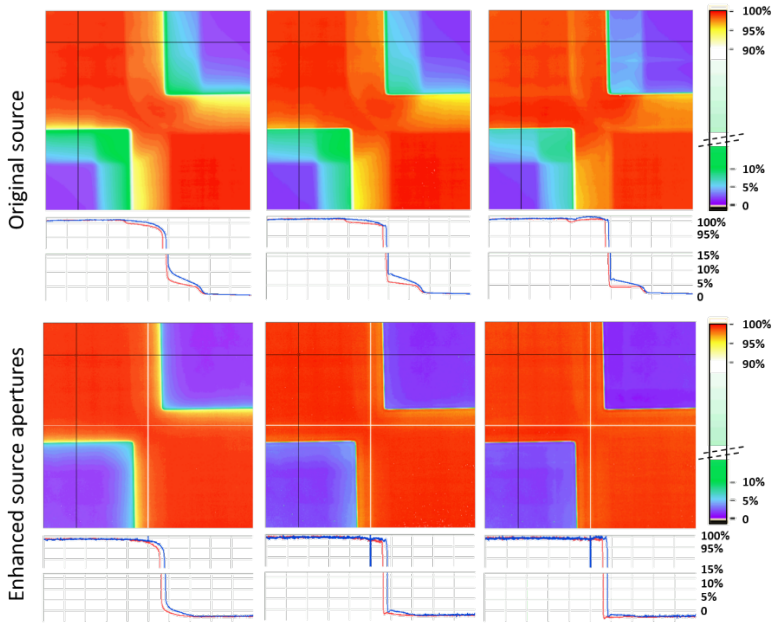

Figure 26: Results of the image correction method. (left) initial image, (middle) after PSF deconvolution, (right) after additional corona deconvolution. Profiles are taken along the blue lines.

A suppression of the effects, in the case of the light transport by a factor of 10, and in the case of the gain-drift by a factor of five, has been realised with PTB's CT system by deconvolution. Besides the numerical correction, a suppression of the corona effect by a factor of 10 was possible by a constructive enhancement of the source's aperture. The influence of the respective correction methods is demonstrated in Figure 26. It is recommended to firstly take advantage of constructive means and secondly utilise calculational corrections. The numerical model is less stable as it contains several geometrical parameters. The removal of the coronas by modified apertures could be demonstrated at the CT-system of METAS as well.

Artefacts originating from scatter radiation were examined by Monte Carle simulations. EMPA, with its simulation framework, investigated scattering originating in the sample object, the entrance window of the detector, the detector material (scintillator) itself and the silicon attached at the back. The simulation results

are showing that dominant sources of scattering are in the entrance window of the detector and the material attached on the back of the detector. Object scattering is strongly related to its geometry and orientation.

Deviations from the assumed scan trajectory generally result in motion-blur artefacts. Reconstruction software that uses individual projection matrices is suitable for taking known deviations into account and for reducing corresponding artefacts. Deviations from the standard trajectory have been characterised by METAS and VTT for their CT systems. Thermal modelling, as done by FSB, is another source to describe deviations. BAM used the rotary table characterisation by VTT to show the potential artefact reduction for a simulated example. A virtual setup with METAS's corner cube has been defined, which includes the angular and position deviations of the rotary table during its rotation. The standard CT reconstruction, considering an ideal circular trajectory, results in blurred volume data as shown in Figure 27 (top right). Figure 27 (bottom right) presents a much sharper image of the reconstructed volume. This volume was reconstructed using the same Feldkamp implementation, but with individual projection matrices that account for the deviations of the turntable as it rotates. The accuracy of the sample surface determined in the volume data with respect to the original geometry used for the simulations was improved by a factor of four by reconstructing with the exact trajectory.

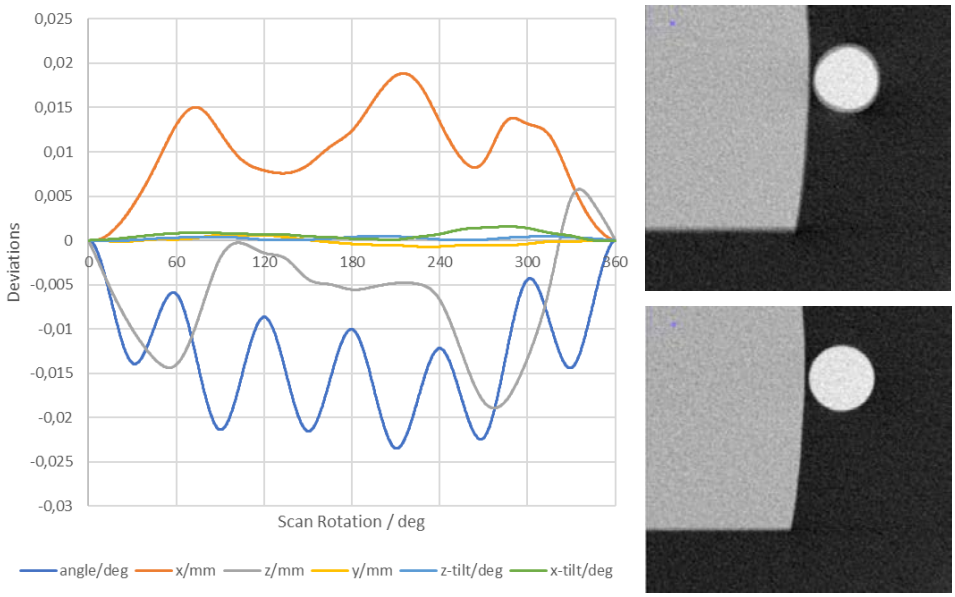

Figure 27: Rotary table characterisation by VTT (left), and virtual CT, result of Feldkamp reconstruction with standard circular trajectory (top right) and circular trajectory including known deviations (bottom right).

Simulation campaign and uncertainty evaluation

UoS performed uncertainty propagation experiments on the influence of photon count and number of projections. UoS generated four initial datasets with real measurements, and six additional data sets were generated by reducing the number of projections from one of these scans, using the full low noise data as the basis. Additional Poisson noise was also added to the data to simulate data collected using fewer photons for each pixel, providing an additional three datasets. The simulated radiographs were batch-reconstructed using three different methods, the FDK, CGLS and FISTA-TV algorithms, providing thirty-nine sets of volumetric images for metrological analysis, which show the uncertainty of the considered measurement task from the simulations.

A full-scale Monte-Carlo simulation has been run by BAM in aRTist to determine the required number of photons for the approximate scatter simulation. The correlation function of single projection scatter images from various photon numbers with a reference scatter image from a very large number of photons ($4.5 \cdot 10^{13}$ photons) was studied. BAM found that aRTist scattering simulation with 10^7 to 10^8 photons provides sufficiently high correlation with a full Monte-Carlo scattering simulation (10^{13} photons).

Additionally, the effect of the photon number in the aRTist scattering simulation on the dimensional measurements was evaluated using the Multi-Geometry Cuboid made of aluminium and iron. Several full CT scans with different numbers of photons (10^5-10^9) for the scatter image approximation were simulated in aRTist

and compared to the reference simulated CT scan with 10^{10} photons. BAM showed that for both investigated materials the geometry deviation reduces almost to zero with the number of photons higher than 10^6 for aRTist's scatter image approximation.

More than fifty virtual CT scans have been simulated by BAM using the AdvanCT module of aRTist and have been batch reconstructed using a FDK algorithm. Two scenarios were used, provided by METAS and FAU. The simulations were partially run at the IRIDIS supercomputer of UoS.

PTB applied aRTist's new AdvanCT-Module to simulate fast CT scans with arbitrary trajectories. The trajectory was devised by CEA in WP3 and used on their CT scanner with robotic manipulators. Fifty repeat simulations were performed with additional variations of the nominal geometry. The variations were based on the typical positional inaccuracy of robotic arms. The test object for this simulation campaign was the LNE step cylinder developed in Objective 1. The reconstructions of the acquired projection data were supposed to be done using state-of-the-art iterative reconstruction algorithms of the TIGRE Toolbox. However, due to incompatibilities, the trajectory could not be implemented in the TIGRE Toolbox despite the help of UBATH. The quality of results from other reconstruction software was not high enough to allow for an uncertainty evaluation. The low quality is due to the limited angle range covered by the trajectory which leads to very high noise along the angle range not covered. This noise completely obscures the surface of the object in many places.

VTT analysed the uncertainty of the XCT surface roughness measurements performed in Objective 2, where one sample was measured with a voxel size of approximately 20 µm by VTT, NPL and UNOTT. The dataset was aligned using the spheres within the sample. The sphere-to-sphere distances were also used to study magnification errors. Surface data was extracted in point cloud format from the XCT-measurements at a pixel spacing of approximately 20 µm.

For analysis of the uncertainty of roughness measurements the work was split into two parts. First, the analysis was focused on how well the measured surface represents the real surface. Several real and simulated measurements were done, volumetric data was analysed and surfaces calculated with slightly varying parameters. Then the knowledge from the first part was used to select a relevant subset of the measured data for analysis of the uncertainty of the roughness parameters.

The conclusion of this work is that measurement and sampling methods have relatively small effect on the surface texture parameters measured for this 3D printed sample, where roughness is analysed on a horizontal scale of 80 µm to 800 µm or 2500 µm. Simulated measurements suggest that there might be is a small "bias effect" caused by XCT imaging that is independent of scale error and repeatability. This, however, is in the same magnitude as the variability of the measurements.

In summary, simulations could be effectively applied for uncertainty estimation of dimensional XCT measurements with standard circular and arbitrary trajectories, and also for XCT surface roughness measurements. Fast approximate scatter simulations were validated against full Monte-Carlo simulations. Influences on the measurement uncertainty could be studied by Monte-Carlo simulations. However, further research is needed on the modelling of XCT systems and the processing of the Monte Carlo simulations to improve the applicability of the simulation-based uncertainty determination.

Summarising the results of the work on objective 4, the integration of the simulation into the dimensional XCT measurement process initially created the basis for further investigations.

To determine accurate model parameters for the simulations, four reference objects have been developed by METAS and PTB, and were calibrated by METAS, Werth and FAU, to be used for comparisons of Monte-Carlo simulations with real measurements. The aim of the task was fully achieved by successfully testing procedures for model adaptation. The reached automation of the determination of accurate model parameters underlines this achievement.

The aim to develop correction methods for specific CT image forming artefacts was fully achieved by demonstrating the suppression of several effects, as scattering apertures, visible light transport in the detector's scintillator, and burn-in. Additionally, a rotary table characterisation was successfully used during reconstruction to reduce motion-blur from a non-ideal scan trajectory.

With the exception of comparing a simulation-based uncertainty assessment with empirical measurements, the simulation campaign and uncertainty evaluation were successful and the objective was achieved.

5 Impact

Project results have been presented in 36 presentations and posters at national and international conferences and an additional seven are planned in 2022 including specialised CT events such as Dimensional X-ray Computed Tomography (dXCT) 2018, 2019, 2020, 2021 and the Conference on Industrial Computed Tomography (ICT) 2019, 2020 and 2022. Other invited presentations have also been given at the Micro and Nanotomography Symposium: 3D Imaging for Industry in Switzerland and the Seminar Series in XCT in the UK.

Fourteen open access publications and proceedings have been published and an additional eight have been submitted by the consortium. Further to this the project's website was regularly updated and is available at www.ptb.de/empir2018/advanct

Impact on industrial and other user communities

The results of this project can be used by a broad range of end users in industry such as manufacturing (in particular manufacturers of plastic parts fabricated by injection moulding), microfabrication (e.g. watch parts), automotive (e.g. cast parts, electronic components, fuel injection components), telecommunication (e.g. fibre-optic and high frequency connectors), medical (e.g. ophthalmology, dental implants), pharmaceutical (e.g. lab on a chip), and metrology service providers.

The project's significant improvements in the measurement accuracy and timeframe of CT measurements (objectives 1, 3 & 4) will be of particular interest to industrial end users, who are in urgent need of inline CT measurements and better quality control. Similarly, the potential use of CT to evaluate surface roughness (objective 2) promises to greatly benefit manufacturing.

The project has engaged directly with industry through its stakeholder committee which included members from Nikon Metrology Europe NV, Messtronik GmbH and The Manufacturing Technology Center. The consortium also included industrial partners Bosch, LEGO, NovoNordisk, Volume Graphics (VG), Werth Messtechnik, Yxlon International and Carl Zeiss, who participated in case studies to demonstrate the direct applicability and benefits of the project's improved CT measurements. The case studies include (i) NovoNordisk – The relationship between surface roughness and flow rate in small bore needles, (ii) LEGO – 3D surface texture parameterisation of small internal bores for mould tool conformal cooling and (iii) Bosch - traceable CT measurement of automotive parts.

To help disseminate the project's results to industrial end users the project collaborated with the dXCT society and hosted a workshop on "Advanced XCT for dimensional metrology- reconstruction algorithms" in December 2020. The workshop disseminated the latest developments in the reconstruction of XCT to more than 80 participants from 38 different organisations (11 universities and 27 commercial companies or research institutes worldwide).

Further to this the project has produced articles for end users on CT in METinfo and IEEE Transactions, as well as a promotional video on Computed tomography "Small parts reveal their shape" (https://youtu.be/e3pGsZK1jLI)

Impact on the metrological and scientific communities

The main impact of this project for the metrological and scientific communities will be the provision of traceability for CT measurements and an increase in their accuracy. To support this the project has hosted a workshop at The European Society for Precision Engineering and Nanotechnology (euspen) on Uncertainty in dimensional XCT. The euspen workshop attracted approximately 50 participants from industry and science.

The results will also enable NMIs to introduce new CT calibration services at partners PTB, VTT and METAS. Indeed, VTT has already started to provide XCT measurement services for industrial components and METAS has launched dimensional XCT feasibility studies and first services for end users.

The reference standards developed in objective 1 are being used for calibration of measurements (at VTT). Thus, the accuracy of measurements, where pre-existing standards were unsuitable, could be increased.

Further to this, the project has created impact through the uptake of the accuracy improvements by users from outside of the consortium who aim to improve their hardware and software. To support this the project has provided training to the scientific community on high-end industrial CT Software 'VG STUDIO MAX and VG in

LINE - improved and efficient use' and 'Using simulator aRTist' (objective 4). The improved TIGRE software (objective 3) is freely available and open source.(https://github.com/CERN/TIGRE)

Impact on relevant standards

This project enabled better comparison of CT systems by providing input to improved standardised testing procedures. Unlike current standardised test procedures which only include geometrical measurements of existing or developmental monomaterial objects, this project provided input on test procedures that take multimaterial objects and surface roughness evaluation into account.

The project provided input to and helped to accelerate the establishment of ISO standards within the field of CT for geometrical measurements of monomaterial and multimaterial objects. Indeed, the project liaised with ISO TC213 WG10 "Coordinate measuring machines", ISO TC 261 "Additive manufacturing".

In addition, the project has provided input to standardisation bodies such as ISO TC213 WG10 (Coordinate metrology) BIPM CCL (Length), VDI/GMA FA 3.33, DIN NA 152-03-02-12 UA KMT (Coordinate metrology), ASTM E07 (Nondestructive Testing) and METSTA GPS (a national GPS group).

Longer-term economic, social and environmental impacts

The long-term impact of this project will be through the support of European manufacturers (e.g. in the automotive and healthcare industry), who require advanced measurement capabilities for quality control and development. In addition, the project's advanced CT measurement capabilities, (e.g. the measurement of complete workpiece geometry, without damage, within a shorter timeframe) should also support the development of new production technologies for electro- and mechanical components.

The project's support for the increased use of industrial CT systems will help to strengthen the market position of European CT manufacturers. Currently, four of the top five manufacturers in the world market for CT dimensional metrology are European.

Better CT measurements should lead to higher quality, longer-lasting products and the improvement of the safety of household appliances parts for the automotive industry and medical products. The case studies investigated in this project illustrate the broad range of applications of CT. They include healthcare products for insulin injection (a life-saving application) and LEGO toys that have inspired creativity in children (and adults) for generations.

By increasing end users' confidence on CT measurements, this project will help to increase the use of CT in industry and hence improve product development and processes. The use of traceable XCT measurements in quality assurance and quality control should also lead to earlier detection of defective parts. Hence chances to reuse materials and components would increase, thereby improving efficiency and reducing waste. For example, the emissions of combustion engines are dependent on the dimensional characteristics of fuel injection systems. Therefore, better measurements of fuel injection system components should lead to reduced emissions.

6 List of publications

[1]. Bircher, B.A. et al., *CT geometry determination using individual radiographs of calibrated multi-sphere standards*, Proceedings iCT - 9th Conference on Industrial Computed Tomography, 2019 https://www.ndt.net/article/ctc2019/papers/iCT2019_Full_paper_43.pdf

[2]. Bircher, B.A. et al., *CT machine geometry changes under thermal load*, Proceedings iCT - 9th Conference on Industrial Computed Tomography, 2019, https://www.ndt.net/article/ctc2019/papers/iCT2019_Full_paper_47.pdf

[3]. Obaton, A.-F., et al., *Reference standards for XCT measurements of additively manufactured parts*, iCT - 10th Conference on Industrial Computed Tomography, 2020, https://www.ndt.net/article/ctc2020/papers/ICT2020_paper_id152.pdf

[4]. Katic, M. et al., *Investigation of temperature-induced errors in XCT metrology*, International Journal of Automation Technology, https://doi.org/10.20965/ijat.2020.p0484

[5]. Biguri, A. et al., *Arbitrarily large iterative tomographic reconstruction on multiple GPUs using the TIGRE toolbox*, Journal of Parallel and Distributed Computing, https://arxiv.org/abs/1905.03748

[6]. Bircher, B.A. et al., *X-ray source tracking to compensate focal spot drifts for dimensional CT*

measurements, Proceedings iCT - 10th Conference on Industrial Computed Tomography, 2020, https://www.ndt.net/article/ctc2020/papers/ICT2020_paper_id110.pdf

[7]. Bircher, B.A. et al., METAS-CT: *Metrological X-ray computed tomography at sub-micrometre precision*, Proceedings euspen's 20th International Conference & Exhibition 2020, https://www.euspen.eu/knowledge-base/ICE20131.pdf

[8]. Chrétien, S., et al., *Efficient hyper-parameter selection in total variation-penalised XCT reconstruction using Freund and Shapire's Hedge approach*, Mathematics, https://doi.org/10.3390/math8040493

[9]. Küng, A. et al., *Low-Cost 2D Index and Straightness Measurement System Based on a CMOS Image Sensor*, Sensors, https://doi.org/10.3390/s21020591

[10]. Lohvithee, M. et al., *Ant Colony Based HyperParameter Optimisation in Total Variation Reconstruction in XCT*, Sensors, https://doi.org/10.3390/s19245461

[11]. Thompson, A. et al., *Calibration of X-ray computed tomography for surface topography measurement using metrological characteristics*, Proceedings euspen 2020, https://www.euspen.eu/knowledge-base/ICE21165.pdf

[12]. Bircher, B. et al., *Measurement of temperature induced X-ray tube transmission target displacements for dimensional computed tomography*, Precision Engineering, https://doi.org/10.1016/j.precisioneng.2021.06.002

[13]. Chrétien, S. et al., *Fast hyperparameter calibration of sparsity enforcing penalties in Total Generalised Variation penalised reconstruction methods for XCT using a planted virtual reference image*, Mathematics, https://doi.org/10.3390/math9222960

[14]. Sun, W. et al., *Establishment of X-ray computed tomography traceability for additively manufactured surface texture evaluation*, Additive Manufacturing, https://doi.org/10.1016/j.addma.2021.102558

[15]. Obaton, A.-F, et al., *Comparison campaign of XCT systems using machined standards representative of additively manufactured parts*, Proceedings of the 11th Conference on Industrial Computed Tomography (iCT) 2022, https://www.ndt.net/article/ctc2022/papers/ICT2022_paper_id207.pdf

[16]. Bircher, B., et al., *Traceable determination of non-static XCT machine geometry: New developments and case studies*, Proceedings of the 11th Conference on Industrial Computed Tomography (iCT) 2022, https://www.ndt.net/article/ctc2022/papers/ICT2022_paper_id209.pdf

[17]. Rathore, J., et al., *Benchmarking of different reconstruction algorithms for industrial cone-beam CT*, Proceedings of the 11th Conference on Industrial Computed Tomography (iCT) 2022, https://www.ndt.net/article/ctc2022/papers/ICT2022_paper_id244.pdf

[18]. Sun, W., et al., *Evaluation of X-ray computed tomography for surface texture measurements using a prototype additively manufactured reference standard*, Proceedings of the 11th Conference on Industrial Computed Tomography (iCT) 2022, https://www.ndt.net/article/ctc2022/papers/ICT2022_paper_id260.pdf